MDPI

Article

Field Measurements of Tree Dynamics with Accelerometers

Andrea Giachetti [1,*], Giacomo Zini [1], Yamuna Giambastiani [2] and Gianni Bartoli [1]

1   Department of Civil and Environmental Engineering, University of Florence, 50139 Florence, Italy
2   National Research Council, Institute of Bioeconomy, 50019 Florence, Italy
*   Correspondence: andrea.giachetti@unifi.it

Abstract: A comprehensive understanding of the dynamic behavior of a tree can play a key role in the tree stability analysis. Indeed, through an engineering approach, the living tree can be modeled as a mechanical system and monitored observing its dynamic properties. In the current work, procedures of dynamic identification used in civil engineering are applied to the case study of a black locust (*Robinia pseudoacacia* L.). The tree was instrumented with 13 seismic, high-sensitivity accelerometers. Time histories of the tree response under ambient vibration were recorded. Three representative sections of the trunk (the collar, the diameter at breast height, and the tree fork) were equipped with three accelerometers, in order to obtain lateral and torsional vibrations. Moreover, two pairs of accelerometers were fixed on the two main branches. The results show that it is possible to identify the natural frequencies of a tree under ambient vibrations, thanks also to the support of a preliminary finite element model. Even though the optimal position is under the tree fork, the sensors fixed at the diameter at breast height allow a clear identification of the main peaks in the frequency domain.

Keywords: tree dynamics; tree stability; tree monitoring; ambient vibration tests (AVTs)

1. Introduction

Urban trees and forests produce multiple benefits for citizens, thanks to their functionality in ecosystem services [1,2]. In recent years, a growing interest in the arboreal heritage and vegetation has been witnessed, through planning actions for new plants, greater care, and monitoring at birth. In addition, the foundation and participation of associations aimed at the protection of urban green has increased [3–10]. On the other hand, the scientific community is active in implementing ever-better systems to monitor the urban plants' health, helping the owners to keep the city safe. Particular attention to the safety of places also derives from the increase in extreme weather events [11]. Indeed, from a natural risk perspective, the trees can be considered as vulnerable elements of an urban system that can cause damage to things and people [12–14].

One of the duties of the modern arboriculture is the health and stability monitoring of trees: an activity carried out by professionals with increasingly standardized protocols and procedures in order to reduce the subjective component of the evaluation. Technology and experience have led to a good level of in-depth analysis regarding the evaluation of the health state of the aboveground portions. For instance, by means of tools such as the dendrodensimeter and the sonic tomography, it is possible to accurately investigate the wood degradation and therefore the mechanical functions of the stem [15–17]. Despite the development of sophisticated tools (such as radar, e.g., [18]), the underground portion still presents many uncertainties; indeed, the root systems are not directly investigable and indirect investigation systems have not yet been developed that allow rapid analysis and evaluation [19]. This leads researchers to develop innovative stability monitoring techniques, especially for the assessment of root anchoring and relations with external events (wind, rain, snow, anthropogenic actions, pathogens, etc.). Generally, the technique most used today to evaluate the resistance to overturning of a tree is the controlled pulling test (e.g., [20]), but, due to the great variability of potentially influencing parameters (soil

conditions, distribution of the root system, presence of prevailing winds, etc.), many uncertainties are involved [21]. Therefore, it seems clear that an increasingly in-depth comprehension of the tree stability can be achieved only by facing the tree monitoring with a multidisciplinary approach. In this perspective, the paper aims to investigate the tree dynamics using procedures based on those used in civil engineering.

By means of an engineering approach to the tree biomechanics, especially to the tree stability, a tree can be considered as a "living" structure, and therefore modeled as a mechanical system. Thus, the structural health monitoring methods available for the many civil structures can be used to assess the structural integrity of the trees by means of long-term dynamic monitoring systems. In particular, the development of robust identification techniques [22–25] under ambient vibration have renewed the attention on this topic, and the application of dynamic monitoring systems has become widespread for large civil structures [26–28]. To date, the applications of such methods on trees have not been profoundly investigated yet. In particular, the dynamic response of the trees under ambient vibrations, such as microtremors, light wind, etc., through an operational modal analysis approach, has not been fully analyzed by the scientific community. For instance, Baker [29] investigated the dynamic behavior both in summer and winter time of lime tree by measuring the velocity with a laser-Doppler interferometer. A total of 62 trees were tested, identifying a range of frequencies within the range 0.3–1.5 Hz by performing a conventional fast Fourier transform on the collected time histories. Nonetheless, the tree dynamic was characterized only by the first frequency while the identification of higher resonant frequencies was neglected. Schindler [30] measured the wind-induced vibration on a group of Scots pine trees with biaxial clinometers, indirectly measuring the displacements. The dynamic identification of the trees was performed by means of peaks in the estimated mechanical transfer function, obtaining a range between 0.26–0.34 Hz for the first natural frequency. However, as emerged from the literature [31], there are still many open issues on the tree dynamics.

The current paper deals with the dynamic response of a black locust (*Robinia pseudoacacia* L.) under ambient vibration through the direct measurement of the accelerations along the trunk and the main branches. Starting from preliminary finite element (FE) models of the tree, an experimental layout of 13 high-sensitivity accelerometers was defined. Then, the results of the experimental dynamic testing campaign are presented, showing how a spectral analysis can be a useful tool for a first dynamic identification of the tree. The results presented here are a first step of a wider research; therefore, additional field measurements and further post-processing analyses will be performed in the future. The results indicate an extremely complicated field of research, but they are encouraging for further studies of the topic. Indeed, the operational modal analysis approach can make a significant contribution to the development of advanced monitoring systems, based on the creation of IoT (Internet of Things) devices equipped with high-frequency accelerometers for widespread monitoring of tree stability [32–34].

2. Materials and Methods

2.1. Site and Case of Study

The fieldwork was carried out in the Lastra a Signa countryside (Florence), on a plot of land on a farm (Figure 1). The investigated tree is a black locust (*Robinia pseudoacacia* L.), which grows within a belt of vegetation on the border of an arable field (43°45′50.3″ N; 11°06′44.1″ E). The young plant (about 17–20 years of age) does not show structural defects, such as cavities or caries of the stem and branching, which could alter its behavior. It has a fork of the main stem, which is divided into two branches. The angle of insertion of the branches is less than 30° and there is no inclusion of bark. The crown, in good vegetative conditions, is in contact with the adjacent plants, and has a codominant position, as it receives more light from above than from the sides. It is more exposed to southern winds and is greatly influenced by the presence of adjacent trees, participating in the canopy structure. The selected tree was not protected by legal constraints (such as public

or monumental trees), and it was in a safe place if during the tests an unexpected failure occurred. The tree is a portion of a linear group of trees, which is a configuration that one can find in the urban environment, for instance, along a boulevard. The stand represents an ecological corridor, has an age of about 15–20 years, and the most representative plant species are maples (*Acer campestre*), ashs (*Fraxinus ornus*), oaks (*Quercus pubescens*), and other black locust plants. The instrumented tree was about 6.9 m high, with a diameter breast height of 15.3 cm and a crown diameter of about 4 m. The measured plant, on the day of the fieldwork (13 October 2021), is in the vegetative phase, with complete foliation. Only a few yellowed leaves are noted due to the approaching phase of vegetative quiescence.
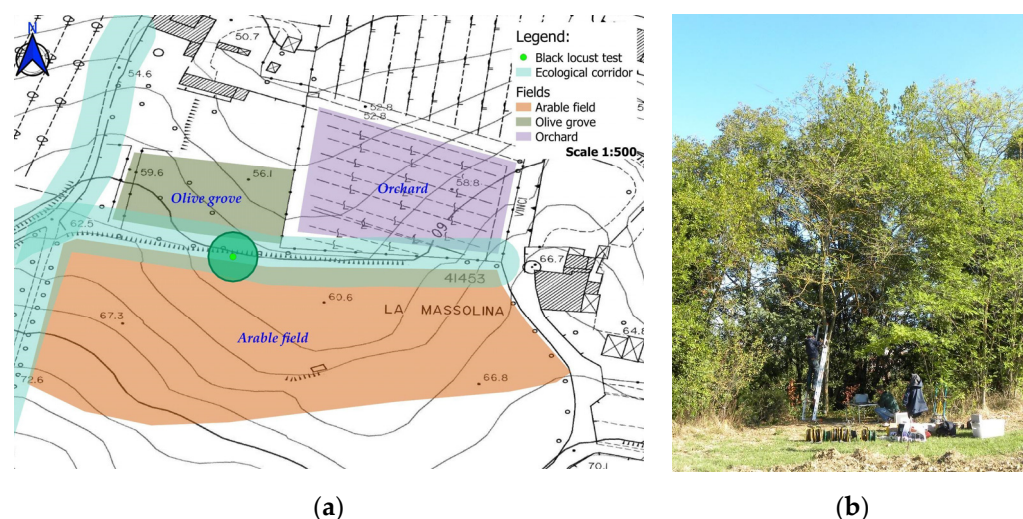

| (**a**) | (**b**) |

Figure 1. An overview of the selected site (**a**) and the tree during the installation of the accelerometers (**b**).

2.2. Analytical Model

To have a first approach to the tree dynamic, a simplified analytical model of a tree with a trunk height h, consisting of a lumped mass system with the canopy approximated as a sphere of radius R_s and a rotational inertia I_0 about the vertical axis, was considered. The flexural stiffness of the trunk $k_\bullet$ (relative to the $\bullet$ axis) can be approximated as a simple cantilever beam. Thus, in both directions it can be expressed as follows:

$$k_{xx} = k_{yy} = 3\frac{EJ_{xx}}{h^3} \qquad with \qquad J_{xx} = J_{yy} \tag{1}$$

Meantime, the torsional stiffness k_θ can be calculated as follows:

$$k_\theta = \frac{GJ_{zz}}{h} = \frac{2EJ_{xx}}{2(1-\nu)h} \simeq \frac{EJ_{xx}}{h} \tag{2}$$

where G is the shear modulus, E is the Young modulus, ν is the Poisson's coefficient, $J_\bullet$ is the moment of inertia about the $\bullet$ axis, and h is the height of the trunk. The translational frequencies for the system can be calculated as follows:

$$f_\theta = \frac{1}{2\pi}\sqrt{\frac{k_\theta}{I_0}} = \sqrt{\frac{5EJ_{xx}}{2M_s R_s^2 h}} \tag{3}$$

where M_{tot} is the total lumped mass, M_s is the canopy mass, and I_0 is the inertia of the tree crown about the vertical axis (approximating it as a sphere). The ratio between the first torsional and bending frequencies can be calculated as follows:

$$\frac{f_\theta}{f_t} = \sqrt{\frac{5M_{tot}}{6M_s}}\left(\frac{h}{R_s}\right) \tag{4}$$

The total mass of the system can be expressed as the mass of the canopy plus one third of the trunk mass M_{tr} (e.g., [35]); the above equation can be simplified as follows:

$$\frac{f_\theta}{f_t} = \sqrt{0.83 + 0.27\frac{M_{tr}}{M_s}\left(\frac{h}{R_s}\right)} \cong \frac{h}{R_s} \tag{5}$$

meaning that, under the above-mentioned assumptions, the ratio between the torsional and the translational frequencies mainly depends on the ratio between the trunk height and the radius of the canopy. Indeed, in this simplified model, if the radius of the tree crown is higher than the trunk height, the first frequency will be torsional; by contrast, if the height of the trunk is higher than the radius of the canopy, the first frequencies will be bending modes about the x–x and y–y axes.

2.3. Preliminary FE model

After some analytical considerations, a preliminary FE model was studied. The FE model was built to gain an idea about the dynamics of the tree and to optimize the sensors layout in the dynamic test campaign. Only the trunk and the two main branches were modeled, considering the higher branches only in terms of mass. As a preliminary strong assumption, the trunk was considered as fixed at the base, neglecting the interaction with the soil.

Using the commercial software SAP2000-v19 [36], the tree was modeled as a discrete dynamic system with beam elements. The properties of the materials were assumed according to the studies of Passialis and Adamopoulos [37,38] and are reported in Table 1. Of course, the mechanical properties of the tested tree can be different from those given in the literature. For instance, Gardiner et al. [39] considered ±20% of variation in the sensitivity analysis of the inputs of two mechanistic models. If the same variation is considered for the mechanical parameters assigned to the numerical model, the frequency f of each mode can be considered the reference value of an interval where $1.225f$ and $0.817f$ are, respectively, the upper and the lower limits.

Table 1. The mechanical properties of each preliminary FE model.

	Model-0	**Model-1**	**Model-2**
Structural mass (kg)	51	71	87
Lumped masses (kg)	108	88	72
Young modulus (MPa)	14,000	14,000	14,000
Density (kg/m^3)	1000	1000	1000

Two different models were used (Figure 2), mainly to understand the influence of the branches in the tree dynamics. Each tree component was modeled with beam elements or additional masses and rotational inertia. Thus, the first model (Model-0) considers only the geometry of the trunk as a beam element, with the upper part of the tree (above the tree fork) modeled as a lumped mass with an assigned torsional inertia. In the second model (Model-1), the trunk and the two main branches are modeled as beam elements, while the remaining parts of the tree (i.e., smaller branches and leaves) are modeled as two lumped masses positioned in the middle of the main branches. To obtain comparable models, the value of the total mass was scaled in order to obtain the same vertical reaction at the base of the tree. Lastly, modal analyses were performed on the three models described above to identify the tree modal properties.

Considering a reference system with the z-axis aligned with the trunk, the plane x–z, which contains the two branches, is named as the lateral plane, while the y–z plane (orthogonal to the lateral plane) is named as the frontal plane. The results obtained from each preliminary FE model are summarized in Table 2. Given the approximation adopted in the preliminary FE models, the comparison between numerical and experimental results

reported in the following section are based on the ratio between the resonant frequencies instead of the mere values.
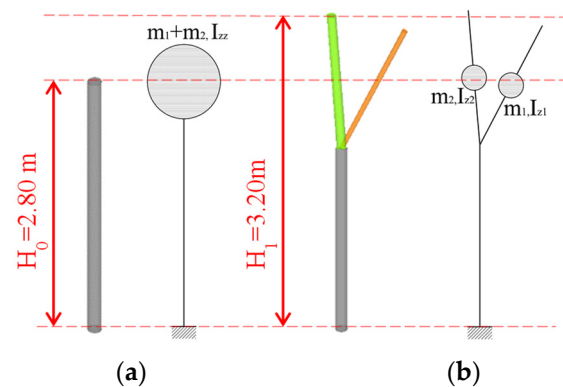

Figure 2. The two preliminary FE models adopted: (**a**) analytical model and the FE models: Model-0, (**b**) Model-1.

Table 2. Results of the preliminary FE models in terms of resonant frequency (f), percentage of participating mass in the x-direction M_x (%), percentage of participating mass in the y-direction M_y (%), percentage of participating mass around z-axis M_z (%), and the sum of the participating mass in each direction ΣM_x (%), ΣM_y (%), ΣM_z (%).

Mode	f [Hz]	M_x [%]	M_y [%]	M_z [%]	ΣM_x [%]	ΣM_y [%]	ΣM_z [%]
Model-0							
I	3.76	88.07	11.93	0.00	88.07	11.93	0.00
II	3.76	11.93	88.07	0.00	11.93	88.07	0.00
III	8.87	0.00	0.00	100.00	0.00	0.00	100.00
Model-1							
I	2.04	68.52	0.00	0.00	68.52	0.00	0.00
II	2.04	0.00	73.81	26.82	68.52	73.81	26.82
III	3.78	0.00	14.44	71.86	68.52	88.25	98.67
IV	3.85	17.32	0.00	0.00	85.84	88.25	98.67
V	15.80	14.16	0.00	0.00	100.00	88.25	98.67
VI	17.33	0.00	11.75	1.33	100.00	100.00	100.00

Clearly, the soil interaction plays a crucial role in the dynamic behavior of the tree. In order to understand such influence, a rotational spring exhibiting different stiffness values was added to Model-0. The results are reported in Figure 3, where the value of the translational frequencies rapidly decay when the spring is softer. In particular, from a stiffness of 10 to 1000 kN · m/rad, a frequency range spanned from 0.5 to 3 Hz is covered. That means that slight differences in terms of the spring stiffness can substantially modify the resonant frequencies of the tree, confirming that for such kind of structural systems, the interaction with soil cannot be neglected to set up reliable models of the tree. In practice, if a pulling test is performed, it is possible to have more reliable boundaries for the rotational stiffness of the tree.

2.4. Experimental Setup

The tested tree was equipped with 13 seismic, high-sensitivity accelerometers (respectively, seven PCB 393-C, two PCB 393-B31, and four 393-B12) measuring the dynamic behavior of five different sections along the trunk and the main branches (see Figure 4).
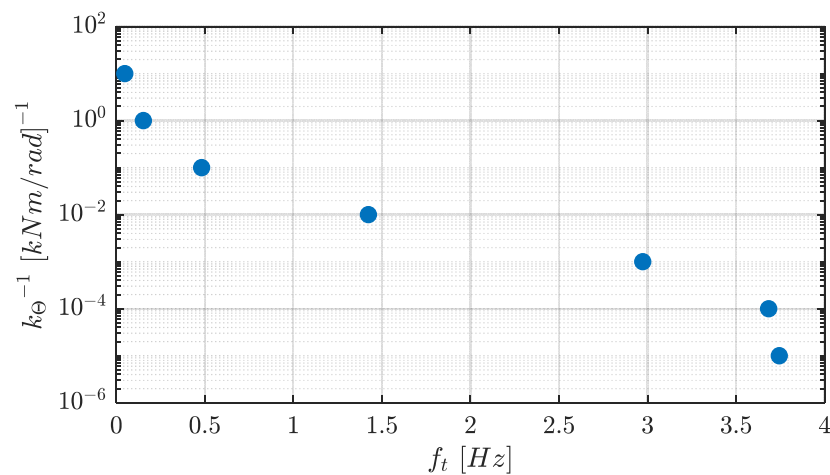
Figure 3. Influence of the rotational flexibility ($1/k_\theta$) on the estimation of the translational frequency f_t.
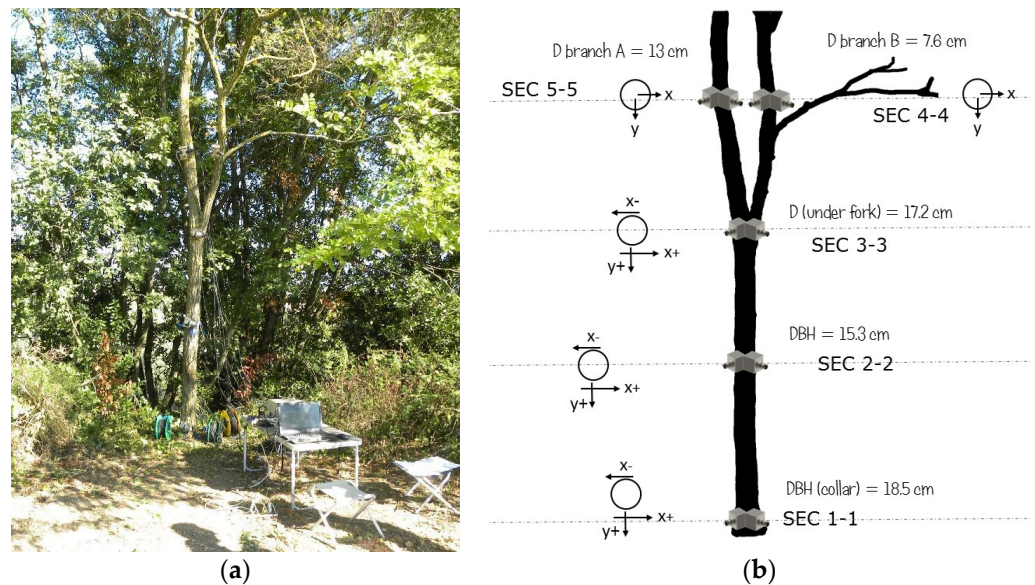

Figure 4. Tree properties and sensor position: (**a**) tested tree; (**b**) sensor layout.

In particular, the trunk was instrumented at three representative heights above the ground level, such as the tree fork (Figure 5a), the diameter at breast height (*dbh*) (Figure 5b), and the collar (Figure 5c). These representative sections were at 2.31 m, 1.3 m, and 0.12 m from the ground, respectively. Each section along the trunk had one sensor along the y-direction (i.e., perpendicular to the frontal plane) and two opposite sensors along the x-direction (perpendicular to the lateral plane) in order to measure possible torsional vibrations. On the branches, only a pair of sensors oriented along the two main directions were fixed at about 0.90 m from the tree fork.

Given that this first experimental campaign was focused on ambient vibration tests (AVTs), the tree was not forced by any external device (i.e., those used for pull and release tests). The tree was forced only by microtremors from the ground and a light wind that, under opportune hypotheses, can be considered as a forcing system with a relatively flat spectrum (e.g., [40]). The field measurements were performed in October, when the environmental conditions were characterized by a sunny day, with temperatures ranging from 25 °C up to 35 °C and light winds. Even if the wind direction and intensity were not measured close to the tree, a check on the weather stations available nearby the selected site confirmed that the wind was at most a light air, according to the Beaufort scale (Figure 6). Eight AVTs were performed, by simultaneously recording all the sensors at a sampling frequency of 4800 Hz for about 30 min, which can be considered a good compromise

for well representing the first resonant frequency and minimizing the noise effects. For instance, applying the rule by Brincker and Ventura ([40]) to a mechanical system with a first resonant frequency of about 0.7 Hz and a damping ratio of 1%, a minimum window length of about 1430 s is attained. Then, in the post-processing phase, the raw signals were filtered with a third-degree Butterworth bandpass filter between 0.15 and 50 Hz.
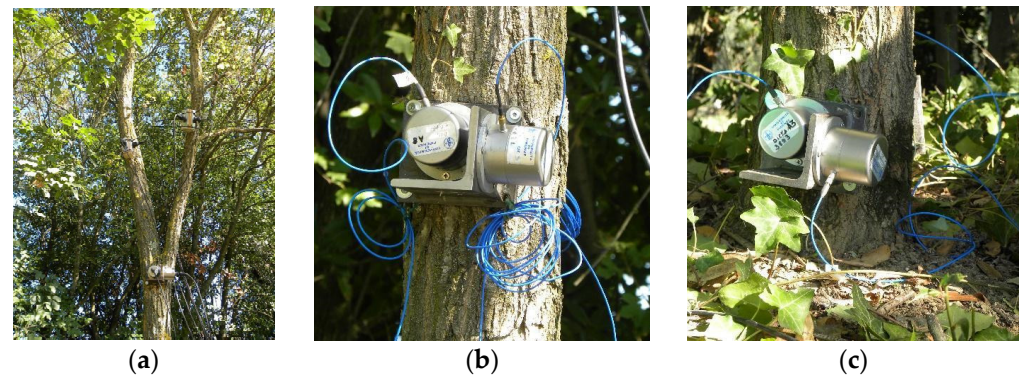

| (**a**) | (**b**) | (**c**) |

Figure 5. Details of the accelerometers fixed on the upper portion of the tree (**a**), at the *dbh* (**b**), and at the collar (**c**).
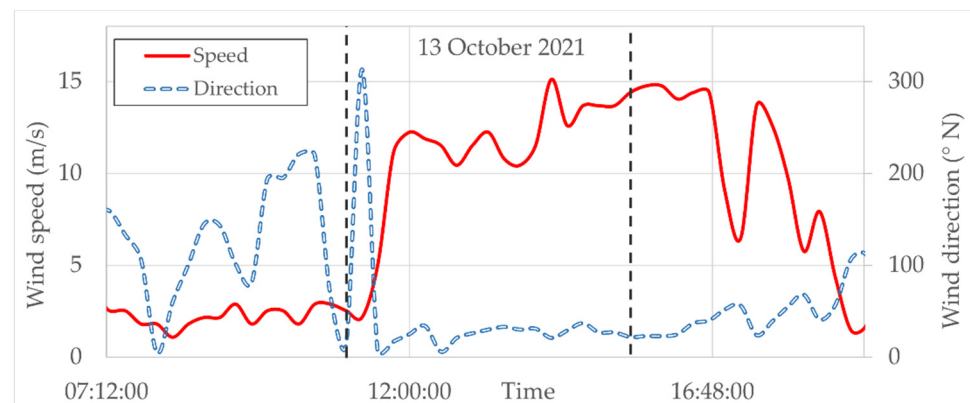

Figure 6. Wind speed and direction from a weather station near the selected site.

3. Results

The current work focuses on the results obtained in the frequency domain. Therefore, power spectral densities (PSDs) of the signals were estimated with the P-Welch algorithm with 50% overlap and using a Hanning window to minimize the leakage effects. In order to improve the clarity of the results, the PSDs obtained on the entire signal were averaged by means of a moving average fitting. An example of the comparison between the results obtained before and after the averaging is reported in Figure 7. Moreover, even if the signal was filtered in the frequency band 0.15–50 Hz, in the following, only the spectra in the range 0.1–5 Hz are shown, where the first resonant frequencies of the tree are supposed to be, according to the purposes of the current work.

Firstly, for each direction, the signals were individually analyzed and compared at different heights along the trunk, corresponding to each measuring station (Section 1-1, 2-2, and 3-3 of Figure 4b). The main results are summarized in Figure 8, where the PSDs obtained for the two orthogonal directions (X and Y) in two different tests are reported. In particular, Figure 8a,b refer to Test #3, performed in the morning when the wind was rarely perceived, while Figure 8c,d refer to Test #8, carried out in the afternoon with an almost constant presence of light wind (Figure 6).
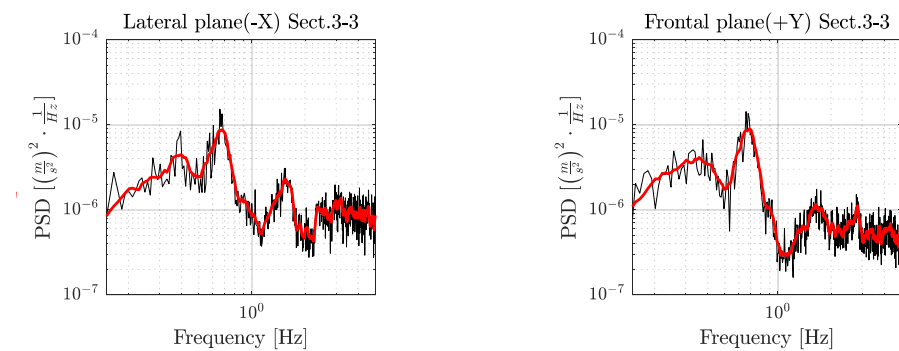
Figure 7. Comparison between the PSDs estimated on the entire signal (**black**) and the PSDs obtained by averaging the signal (**red**).
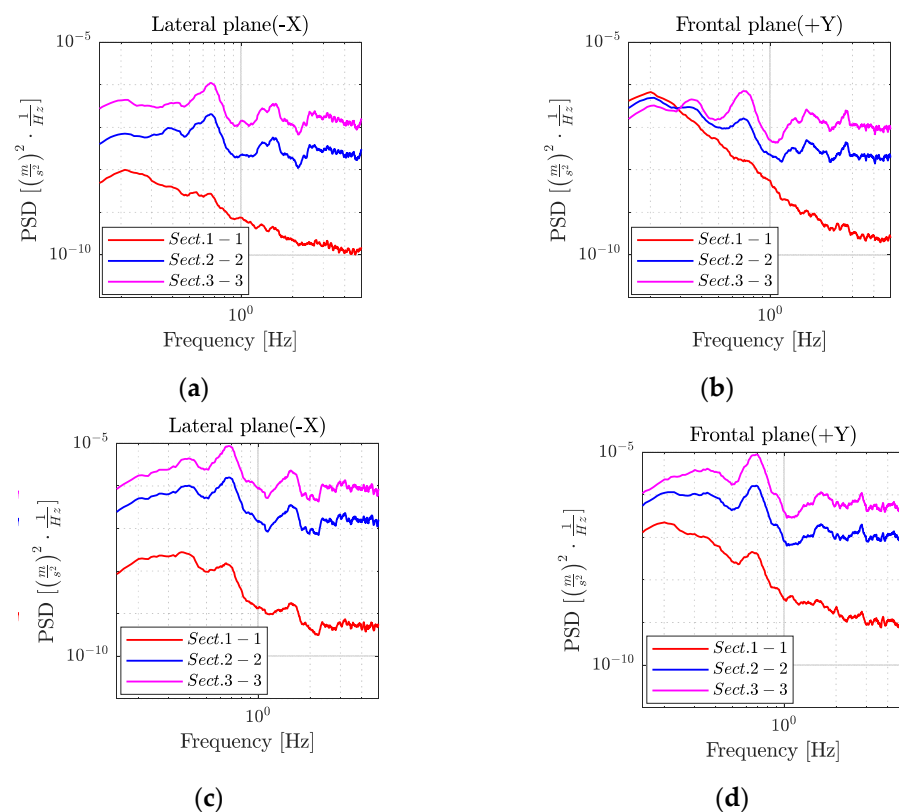

(**a**)　　　　　　　　　　　　　　　　　　　(**b**)

(**c**)　　　　　　　　　　　　　　　　　　　(**d**)

Figure 8. (**a**) The PSDs in the x-direction during Test #3; (**b**) the PSDs in the y-direction during Test #3; (**c**) the PSDs in the x-direction during Test #8; (**d**) the PSDs in the y-direction during Test #8.

The results show a correlation between the sensor position and the energy content in the spectra. In particular, the accelerometers placed under the tree fork can clearly measure vibrations in both directions also in Test #3 (Figure 8a,b), therefore this can be considered an optimal position to measure the tree dynamics. Moreover, the sensors fixed at the *dbh* can also represent the frequency content of the tree sways well, as shown in Figure 8 (Section 2-2). At a first glance, some broadband peaks around 0.7 Hz can be identified in the PSDs, presumably linked with the first resonant frequencies of the tree.

The branches influence the global dynamic of the tree [41]; therefore, the normalized PSDs (NPSDs) of the signals measured in Sections 4-4 and 5-5 were estimated. The NPSDs, with respect to the energy content of the signals, were analyzed on the two main branches to investigate the contribution of each sub-system to the global dynamics of the tree. Such normalization allows the comparison of the spectral content of the two main branches without any distortion due to the energy distribution along each frequency band of the input signal.

The results are shown in Figure 9, where the two global frequencies are confirmed around 0.65–0.7 Hz, and other peaks can be identified between 1–2 Hz and 2–3 Hz.
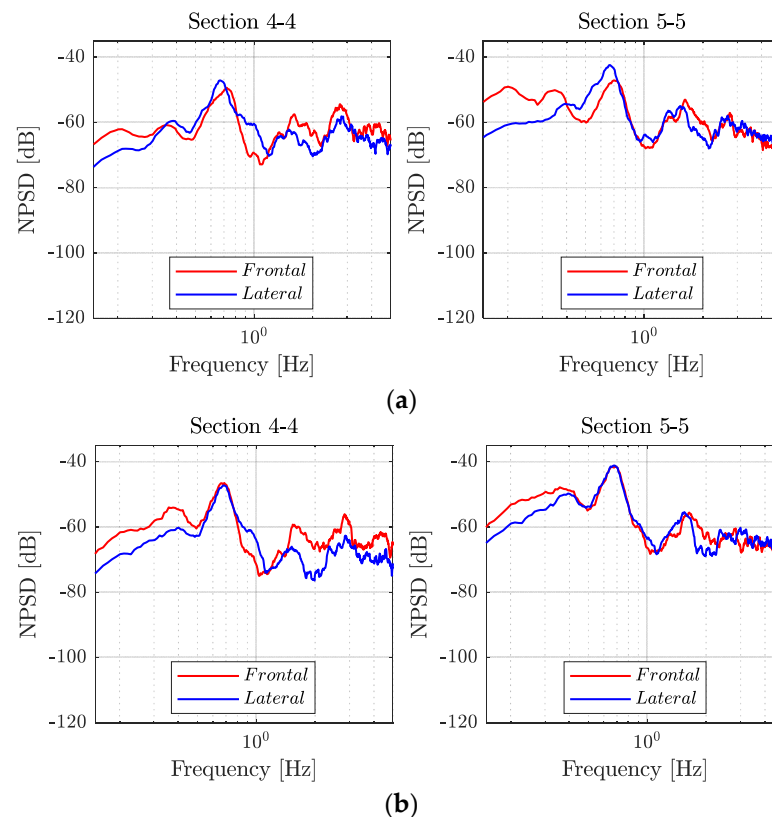

Figure 9. The NPSDs of the two branches in the lateral direction (x) and in the frontal direction (y) during Test #3 (**a**) and Test #8 (**b**).

Lastly, global analyses of the spectral composition by means of the averaged normalized power spectral densities (ANPSDs) [42] for Section 3-3 in Test #3 and Test #8 are reported, respectively, in Figure 10a,b. In particular, the NPSDs of the symmetric (mean of the measured signals along each direction) and antimetric (difference of the measured signals along each direction) component of the signals were evaluated at each measuring station along the tree, giving an idea about the nature of the identified resonant frequencies. Considering Section 3-3 as the most representative to characterize the global dynamics of the tree, only the results of this section are reported herein in Figure 10. While in the range of 2–5 Hz the ANPSD is almost flat in both the considered tests, the first three modes are clearly visible in the frequency band between 0.5–1 Hz, and some other peaks can also be seen in the frequency band between 1–2 Hz.

The results presented in Figure 11 show that, on the one hand, the global dynamics of the tree can be perceived in the two main planes (frontal and lateral) with a uniform amplification of the spectra due to the higher sensor position. On the other hand, the modes with a torsional component around the vertical z-axis are more amplified in the branches than in the trunk. In both the presented tests with different loading conditions (Test #3 and Test #8), the first two modes around 0.7 Hz in the frontal and horizontal plane, respectively, can be clearly detected. In addition, the third mode, exhibiting a predominant torsional component about the vertical axes, can be recognized at a frequency of about 0.8 Hz, while the higher modes in the two considered planes are quite closer at about 1.5 Hz, and the second torsional mode can be probably identified at about 3 Hz. It is worth noting that a slight difference in the frequency domain response can be detected according to the different load conditions. In particular, some broadband peaks below 0.5 Hz can be

identified in both conditions and some additional torsional peaks in the branches PSDs between 1 and 2 Hz can be localized when the wind is almost absent (Figure 11a).
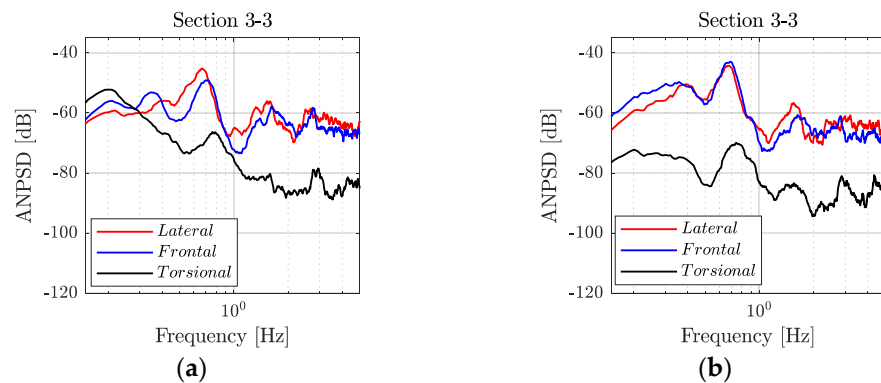

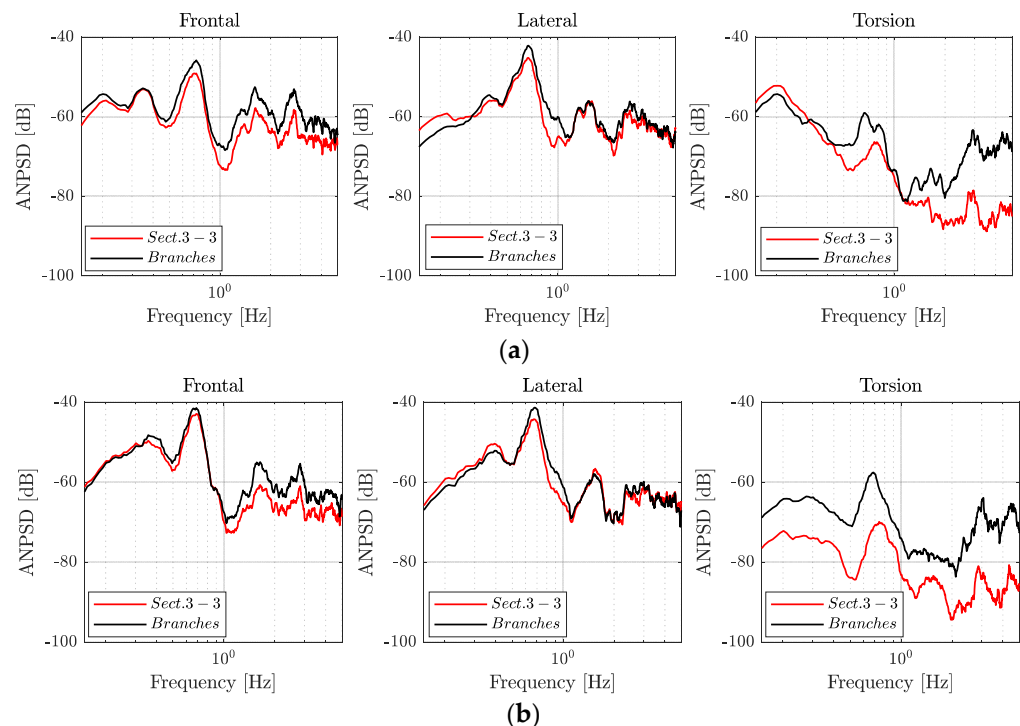**Figure 10.** Frontal (y), lateral (x), and torsional vibrations estimated at Section 3-3 (**a**) in Test #3 and (**b**) Test #8.

Figure 11. The ANPSDs estimated in the trunk (Section 3-3) and on the branches for the considered tests: (**a**) in Test #3 and (**b**) Test #8.

4. Discussion

The extensive experimental campaign performed shows that a dynamic identification of the tree under ambient vibration can be performed with the classical spectral analysis method. If properly combined with a preliminary numerical model, both the estimation of the PSDs of each signal and the ANPSDs of each section along the trunk can provide useful information for the dynamic identification of the tree. The main natural frequencies (i.e., those related to global modal shapes) of the tree can be identified, even if some peaks observed at very low frequency (below 0.5 Hz) require further investigations. Small differences in the spectral response can be seen when considering two tests with different loading conditions (e.g., Test #3 and Test #8). This is probably due to the nonlinearities of the mechanical system studied, but also the intrinsic broadness of the peaks observed that can affect the interpretation of the results.

Concerning the comparison between the results of the field measurements and the preliminary FE model, it is possible to highlight the following points:

- The first two frequencies found in the numerical models are almost the same, activating a major part of the participating mass both in x and y directions. This is due to the geometry of the body studied and it gave a warning of the possible presence of very close peaks in field measurements. Indeed, as confirmed by the results, close peaks were found in the frequency domain and, despite the relatively high spectral resolution, sometimes they appeared as a unique broad peak. The combination of PSDs and ANPSDs was helpful in their identification, adding more information about the nature of the two identified modes.
- If the branches are modeled in the FE model, the main frequencies decrease when the branches are modeled, and the ratio between the first resonant frequency and the others increases, as reported in Table 3. These observations confirm the assumption in the literature [31] of the importance of modeling the tree branches.
- The main role of the FE was to support the definition of the experimental setup, especially of the positions of the sensors. The strong assumptions adopted and discussed in Section 2.3 concerning the tree properties can lead to results different from the experimental measures, also in terms of frequency ratios. In particular, referring to the ratios between the first and the third mode reported in Table 3, the differences are still remarkable. Therefore, if a model-based monitoring approach is of interest, the FE model should consider at least the main branches to well represent the tree dynamics, and it should be calibrated after a first set of measurements.
- In the next studies, the fixed support used in the numerical model will be replaced with a more realistic rotational spring. This will further reduce the gap between the resonant frequencies extracted from the experimental campaign and those obtained by the model.

Table 3. The frequency ratio between the lowest resonant frequency and the others for Model-0, Model-1, and the experimental values in the two loading conditions: (i) absence of wind (Test #3) and (ii) with light wind (Test #8).

Frequency Ratio	Model-0	Model-1	Test #3	Test #8
f_I/f_{II}	1.00	1.00	0.95	0.97
f_I/f_{III}	0.41	0.54	0.82	0.88

Concerning the results of the field measurements, one of the main findings is that the frequency content of the signals measured at the *dbh* are comparable to those under the tree fork. Thus, future research can be oriented to a tree monitoring system (or procedure) such that it does not need a complicated installation of the sensors. Nevertheless, given that the accelerations measured at the branches helped the interpretation of the results, it can be suggested to use a first set of dynamic tests with additional sensors, in order to consider the effects produced by the main branches. In the next steps of the research, more sophisticated OMA analyses (e.g., frequency domain decomposition, stochastic subspace identification, etc.) will be performed to obtain accurate information about mode shapes and damping ratios with different sensor arrangements.

Further investigations are needed to deepen the tree dynamics, focusing on the system nonlinearities. For instance, some points have already emerged in the current work, such as the nature of the peaks below 0.5 Hz and tree–soil interaction that should be deepened to build reliable FE models. Therefore, some additional sensors, such as an anemometer to measure the wind speed in the proximity of the tree, and other activities, such a pull and release test, will be included in the next field measurements to increase the level of the available information on those critical points. However, considering the complexity of the problem, the results gave positive feedback for further studies about the real-time dynamic monitoring of trees and their application in a broader structural health monitoring approach.

5. Conclusions

This paper investigates the dynamic behavior of a standalone tree under ambient vibration. The experimental setup was defined by the analysis of some preliminary FE models, and the accelerations were collected by means of 13 high-sensitivity accelerometers (PCB 393-C, 393-B12, and 393 B-31) placed along the tree and its main branches. The spectral analysis of the signals shows that it is possible to identify the first three resonant frequencies of the tree, and the ANPSD analysis adds some information about the modal shape. Nevertheless, during the experimental tests, the wind was not directly measured and the dynamic interaction with the tree cannot be considered. Thus, the nature of the low-frequency peaks must be investigated with additional tests. Along with the wind measurements during the tests, the rotational stiffness of the tree with pull-out tests must also be considered to update the FE model and to check the experimental results.

These findings open a new scenario in the dynamic monitoring of the tree under AVTs that requires some further investigations to broadly apply such a method in the damage assessment of trees. Then, the application to the long-term monitoring data of wider groups of trees with SHM purposes must be considered in the future.

References

1. Du, H.; Zhou, F.; Cai, Y.; Li, C.; Xu, Y. Research on public health and well-being associated to the vegetation configuration of urban green space, a case study of Shanghai, China. *Urban For. Urban Green.* **2021**, *59*, 126990. [CrossRef]
2. Fletcher, D.H.; Likongwe, P.J.; Chiotha, S.S.; Nduwayezu, G.; Mallick, D.; Uddin Md, N.; Rahman, A.; Golovátina-Mora, P.; Lotero, L.; Bricker, S.; et al. Using demand mapping to assess the benefits of urban green and blue space in cities from four continents. *Sci. Total Environ.* **2021**, *785*, 14723. [CrossRef] [PubMed]
3. Vaccari, F.P.; Gioli, B.; Toscano, P.; Perrone, C. Carbon dioxide balance assessment of the city of Florence (Italy), and implications for urban planning. *Landsc. Urban Plan.* **2013**, *120*, 138–146. [CrossRef]
4. Luvisi, A.; Lorenzini, G. RFID-plants in the smart city: Applications and outlook for urban green management. *Urban For. Urban Green.* **2014**, *13*, 630–637. [CrossRef]
5. Semeraro, T.; Scarano, A.; Buccolieri, R.; Santino, A.; Aarrevaara, E. Planning of urban green spaces: An ecological perspective on human benefits. *Land* **2021**, *10*, 105. [CrossRef]
6. Diluiso, F.; Guastella, G.; Pareglio, S. Changes in urban green spaces' value perception: A meta-analytic benefit transfer function for European cities. *Land Use Policy* **2021**, *101*, 105116. [CrossRef]
7. Knobel, P.; Dadvand, P.; Alonso, L.; Costa, L.; Español, M.; Maneja, R. Development of the urban green space quality assessment tool (RECITAL). *Urban For. Urban Green.* **2021**, *57*, 126895. [CrossRef]
8. Giacinto, J.J.; Andrew Fricker, G.; Ritter, M.; Yost, J.; Doremus, J. Urban forest biodiversity and cardiovascular disease: Potential health benefits from California's street trees. *PLoS ONE* **2021**, *16*, e0254973. [CrossRef]
9. Lee, A.C.K.; Maheswaran, R. The health benefits of urban green spaces: A review of the evidence. *J. Public Health* **2011**, *33*, 212–222. [CrossRef]
10. Carreiro, M.M.; Song, Y.C. *Springer series on Chernobyl: A Policy Response Food Web Management: A Case*; Springer: Berlin/Heidelberg, Germany, 2007; ISBN 9780387353029.
11. Ma, J.; Bai, Y.; Shen, J.; Zhou, F. Examining the impact of adverse weather on urban rail transit facilities on the basis of fault tree analysis and fuzzy synthetic evaluation. *J. Transp. Eng.* **2014**, *140*, 04013011. [CrossRef]
12. Giachetti, A.; Ferrini, F.; Bartoli, G. A risk analysis procedure for urban trees subjected to wind- or rainstorm. *Urban For. Urban Green.* **2021**, *58*, 126941. [CrossRef]
13. Eisenman, T.S.; Coleman, A.F.; LaBombard, G. Street Trees for Bicyclists, Pedestrians, and Vehicle Drivers: A Systematic Multimodal Review. *Urban Sci.* **2021**, *5*, 56. [CrossRef]

14. Coleman, A.F.; Ryan, R.L.; Eisenman, T.S.; Locke, D.H.; Harper, R.W. The influence of street trees on pedestrian perceptions of safety: Results from environmental justice areas of Massachusetts, U.S. *Urban For. Urban Green.* **2021**, *64*, 127258. [CrossRef]

15. Guyot, A.; Ostergaard, K.T.; Lenkopane, M.; Fan, J.; Lockington, D.A. Using electrical resistivity tomography to differentiate sapwood from heartwood: Application to conifers. *Tree Physiol.* **2013**, *33*, 187–194. [CrossRef]

16. Gilbert, G.S.; Ballesteros, J.O.; Barrios-Rodriguez, C.A.; Bonadies, E.F.; Cedeño-Sánchez, M.L.; Fossatti-Caballero, N.J.; Trejos-Rodríguez, M.M.; Pérez-Suñiga, J.M.; Holub-Young, K.S.; Henn, L.A.W.; et al. Use of Sonic Tomography to Detect and Quantify Wood Decay in Living Trees. *Appl. Plant Sci.* **2016**, *4*, 1600060. [CrossRef]

17. Sterken, P. The quest for a unified theory on biomechanical palm risk assessment through theoretical analysis and observation. *Sci. Rep.* **2021**, *11*, 22134. [CrossRef]

18. Bassuk, N.; Grabosky, J.; Mucciardi, A.; Raffel, G. Ground-penetrating radar accurately locates tree roots in two soil media under pavement. *Arboric. Urban For.* **2011**, *37*, 160–166. [CrossRef]

19. Giambastiani, Y.; Errico, A.; Preti, F.; Guastini, E.; Censini, G. Indirect root distribution characterization using electrical resistivity tomography in different soil conditions. *Urban For. Urban Green.* **2022**, *67*, 127442. [CrossRef]

20. Sani, L.; Lisci, R.; Moschi, M.; Sarri, D.; Rimediotti, M.; Vieri, M.; Tofanelli, S. Preliminary experiments and verification of controlled pulling tests for tree stability assessments in Mediterranean urban areas. *Biosyst. Eng.* **2012**, *112*, 218–226. [CrossRef]

21. Giambastiani, Y.; Preti, F.; Errico, A.; Sani, L. On the Tree Stability: Pulling Tests and Modelling to Assess the Root Anchorage. *Procedia Environ. Sci. Eng. Manag.* **2017**, *4*, 207–218.

22. Zini, G.; Betti, M.; Bartoli, G. A quality-based automated procedure for operational modal analysis. *Mech. Syst. Signal Process.* **2022**, *164*, 108173. [CrossRef]

23. Reynders, E.; Houbrechts, J.; De Roeck, G. Fully automated (operational) modal analysis. *Mech. Syst. Signal Process.* **2012**, *29*, 228–250. [CrossRef]

24. Cardoso, R.; Cury, A.; Barbosa, F. A robust methodology for modal parameters estimation applied to SHM. *Mech. Syst. Signal Process.* **2017**, *95*, 24–41. [CrossRef]

25. Neu, E.; Janser, F.; Khatibi, A.A.; Orifici, A.C. Fully Automated Operational Modal Analysis using multi-stage clustering. *Mech. Syst. Signal Process.* **2017**, *84*, 308–323. [CrossRef]

26. Barsocchi, P.; Bartoli, G.; Betti, M.; Girardi, M.; Mammolito, S.; Pellegrini, D.; Zini, G. Wireless Sensor Networks for Continuous Structural Health Monitoring of Historic Masonry Towers. *Int. J. Archit. Herit.* **2021**, *15*, 22–44. [CrossRef]

27. García-Macías, E.; Ubertini, F. MOVA/MOSS: Two integrated software solutions for comprehensive Structural Health Monitoring of structures. *Mech. Syst. Signal Process.* **2020**, *143*, 106830. [CrossRef]

28. Moutinho, C.; Pereira, S.; Cunha, A. Continuous Dynamic Monitoring of Human-Induced Vibrations at the Luiz I Bridge. *J. Bridg. Eng.* **2020**, *25*, 05020006. [CrossRef]

29. Baker, C.J. Measurements of the natural frequencies of trees. *J. Exp. Botany* **1997**, *48*, 1125–1132. [CrossRef]

30. Schindler, D. Responses of Scots pine trees to dynamic wind loading. *Agric. For. Meteorol.* **2008**, *148*, 1733–1742. [CrossRef]

31. James, K.R.; Dahle, G.A.; Grabosky, J.; Kane, B.; Detter, A. Tree biomechanics literature review: Dynamics. *Arboric. Urban For.* **2014**, *40*, 1–15. [CrossRef]

32. Van Emmerik, T.; Steele-Dunne, S.; Hut, R.; Gentine, P.; Guerin, M.; Oliveira, R.S.; Wagner, J.; Selker, J.; Van De Giesen, N. Measuring tree properties and responses using low-cost accelerometers. *Sensors* **2017**, *17*, 1098. [CrossRef]

33. Abbas, S.; Kwok, C.Y.T.; Hui, K.K.W.; Li, H.; Chin, D.C.W.; Ju, S.; Heo, J.; Wong, M.S. Tree tilt monitoring in rural and urban landscapes of Hong Kong using smart sensing technology. *Trees For. People* **2020**, *2*, 100030. [CrossRef]

34. Zorzi, I.; Francini, S.; Chirici, G.; Cocozza, C. The Tree Talkers Check R package: An automatic daily routine to check physiological traits of trees in the forest. *Ecol. Inform.* **2021**, *66*, 101433. [CrossRef]

35. *CNR-DT 207 R1/2018*; Istruzioni per la Valutazione delle Azioni e degli Effetti del Vento sulle Costruzioni. National Research Council: Rome, Italy, 2018. (In Italian)

36. CSI (Computers and Structures Inc.). *SAP2000 v23 Analysis Reference Manual*; Computers and Structures Inc.: Berkeley, CA, USA, 2021.

37. Passialis, C.; Adamopoulos, S. A comparison of three NDT methods for determining the modulus of elasticity in flexure of fir and black locust small clear wood specimens. *Holz Roh Werkst.* **2002**, *60*, 323–324. [CrossRef]

38. Adamopoulos, S. Flexural properties of black locust (*Robinia pseudoacacia* L.) small clear wood specimens in relation to the direction of load application. *Holz Roh Werkst.* **2002**, *60*, 325–327. [CrossRef]

39. Gardiner, B.; Peltola, H.; Kellomaki, S. Comparison of two models for predicting the critical wind speeds required to damage coniferous trees. *Ecol. Model* **2000**, *129*, 1–23. [CrossRef]

40. Brincker, R.; Ventura, C.E. *Introduction to Operational Modal Analysis. B*; John Wiley & Sons, Ltd.: Hoboken, NJ, USA, 2015; pp. 1–360. [CrossRef]

41. Sellier, D.; Fourcaud, T. Crown structure and wood properties: Influence on tree sway and response to high winds. *Am. J. Bot.* **2009**, *96*, 885–896. [CrossRef]

42. Ventura, C.E.; Felber, A.J.; Stiemer, S.F. Experimental investigations of dynamics of Queensborough Bridge. *J. Perform. Constr. Facil.* **1995**, *9*, 146–155. [CrossRef]